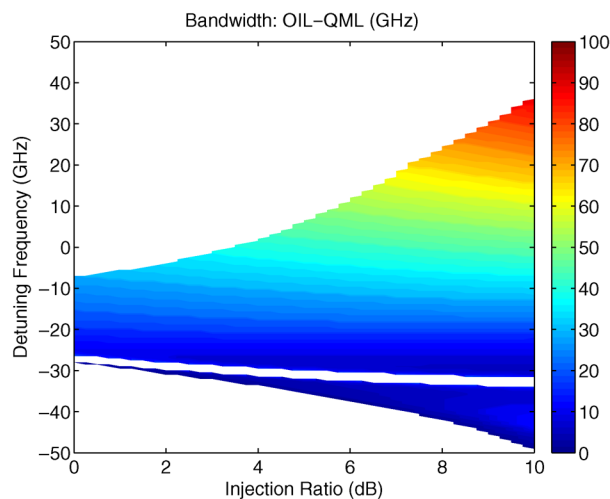


High-Speed Q-Modulation of Injection-Locked Semiconductor Lasers

Volume 3, Number 5, October 2011

X. Wang, Student Member, IEEE
L. Chrostowski, Member, IEEE



DOI: 10.1109/JPHOT.2011.2170159
1943-0655/\$26.00 ©2011 IEEE

High-Speed Q-Modulation of Injection-Locked Semiconductor Lasers

X. Wang, *Student Member, IEEE*, and L. Chrostowski, *Member, IEEE*

Department of Electrical and Computer Engineering, University of British Columbia,
Vancouver, BC V6T 1Z4, Canada

DOI: 10.1109/JPHOT.2011.2170159
1943-0655/\$26.00 ©2011 IEEE

Manuscript received September 1, 2011; revised September 21, 2011; accepted September 22, 2011. Date of publication October 3, 2011; date of current version October 18, 2011. This work was supported in part by the Natural Sciences and Engineering Research Council of Canada. Corresponding author: X. Wang (e-mail: xuw@ece.ubc.ca).

Abstract: We propose a novel approach for high-speed direct modulation of optically injection-locked semiconductor lasers by modulating the photon lifetime (or the Q-factor). Based on the injection locking rate equations, the frequency response is analytically derived and numerically simulated. Compared with conventional current modulation for injection-locked lasers, Q-modulation has the same resonance frequency, but the dc-to-resonance roll-off caused by the real-pole frequency is largely eliminated, and the response beyond the resonance frequency decays much slower; therefore, a significant enhancement in the modulation bandwidth can be achieved. We also show that the two modulation methods have similar chirp characteristics.

Index Terms: Semiconductor lasers, injection-locked lasers.

1. Introduction

Semiconductor lasers are an integral part of optical communication systems. They serve as optical sources with superior performance including small size, high efficiency, low power consumption, and cost, etc. [1]. To convert electrical information into an optical signal, two approaches are commonly used for optical transmitters: 1) external modulation and 2) direct modulation of lasers. External modulation is typically preferred for long haul and high data rates links, where lasers operate in continuous-wave mode and the chirp is very low. However, external optical modulators are usually very expensive and bulky. Furthermore, external modulation dissipates more power than direct modulation, because the laser is continuously turned on to full power, and the external modulator consumes additional power to operate. In contrast, direct modulation of lasers is a simpler solution and more desirable for short-reach interconnects, in particular, for applications where low cost, small size, and low power dissipation are required.

The conventional method of directly modulating lasers is by varying the pumping current. It is well known that the direct modulation bandwidth is limited by the resonance frequency, due to the relaxation oscillation between the carrier and photon densities inside the laser cavity [2]; therefore, most work concentrates on increasing the resonance frequency. It should also be noted that the modulation response decays as $1/\omega^2$ above the resonance frequency, where ω is the angular modulation frequency. On the other hand, several alternative modulation schemes have been proposed, including 1) direct modulation of the material gain by varying the effective carrier temperature in the active region [3], 2) modulating the optical confinement factor Γ by controlling the

current lateral distribution [4], and 3) control of the photon lifetime (or the Q-factor) in the laser cavity by modulating the mirror reflectivity [5]–[9] or the distributed loss [8]. The above schemes have one common feature in that they all attempt to directly affect the photon density in the laser cavity by modulating a physical parameter other than the pumping current, in contrast to interacting indirectly with the photon density through the relatively slow-varying carrier density via the pumping current [5]. Therefore, it can be expected that these modulation schemes will be faster than the conventional current modulation. Among the aforementioned three schemes, the first one is likely to dissipate a lot of power and requires high threshold currents [5], the second one always results in a dual modulation of Γ and carrier density simultaneously [4]; therefore, the last one is of more interest and can be called Q-modulation [6], [7]. A key challenge for realizing Q-modulation is that the laser wavelength needs to be stabilized. One promising laser structure to achieve this was proposed in [7], which consists of a gain section, a phase section, and a Q-modulator. The Q-modulator is an anti-resonant Fabry–Perot cavity and acts as a reflector of the laser, where the reflectivity is changed by varying the absorption coefficient of the modulator waveguide through current injection or reverse-biased electroabsorption effect. Analyses have shown that Q-modulated lasers (QMLs) have a resonance frequency similar to that found in conventional current-modulated lasers (CMLs); however, the response decays as $1/\omega$ at frequencies beyond the resonance frequency [5], [7], [9]. As a result, Q-modulation allows for a much higher modulation bandwidth than conventional current modulation. It is also shown that the chirp is significantly reduced at high frequencies and decreases with increasing frequency [7], [8]. Finally, a high extinction ratio and a high power efficiency can be achieved [7], [9].

Optical injection locking (OIL) is another technique that can provide many significant improvements for directly modulated lasers [10]. One of the most important improvements is that the resonance frequency can be significantly increased. For example, an enhanced resonance frequency of greater than 100 GHz has been experimentally demonstrated using strong OIL, in both distributed feedback (DFB) lasers and vertical-cavity surface-emitting lasers (VCSELs) [11]. However, the bandwidth of OIL is not only governed by the resonance frequency but also the real-pole frequency, which causes a dc-to-resonance roll-off and often limits the bandwidth well below the resonance frequency (this additional feature is specific to OIL lasers) [12]. To maximize the bandwidth, complex adjustments are usually required for the OIL system. Until now, a record intrinsic 3-dB bandwidth of 80 GHz has been achieved in VCSELs [11]. The extrinsic 3-dB bandwidth, which is limited by the laser parasitics, has also been enhanced up to > 40 GHz in both 1.55- μm DFB lasers and VCSELs [10]. OIL can also reduce the chirp, or even achieve adjustable chirp (both sign and magnitude), and therefore, the fiber transmission distance can be greatly increased [13]. Other benefits that OIL can provide include reduction in the relative intensity noise (RIN) and nonlinear distortion, enhancement in the radio-frequency link gain [14], and single sideband modulation [15].

In this paper, we propose a new modulation method by modulating the photon lifetime of an optically injection-locked laser. We expect that this method can incorporate both advantages of Q-modulation and OIL. Based on our small-signal analysis and numerical simulations, we find that using Q-modulation, the enhanced resonance frequency of OIL lasers is the same as in current modulation; however, the modulation bandwidth is no longer limited by the dc-to-resonance roll-off and, thus, can exceed the resonance frequency without complex adjustments. Additionally, the modulation response beyond the resonance frequency decays much more slowly using Q-modulation than using current modulation, thus resulting in a significant enhancement in the 3-dB bandwidth for OIL lasers. Furthermore, the chirp characteristics will also be discussed.

2. Small-Signal Analysis

2.1. Injection Locking Rate Equations

To analyze the dynamics of OIL lasers, the rate equations model is most commonly used [16] and has been experimentally validated by numerous studies [10]–[13], [17]–[19]. The derivation of the

rate equations begins with the differential equation governing the complex electrical field of OIL lasers [12]:

$$\frac{dE}{dt} = \frac{1}{2}(1 + i\alpha) \left[G(N - N_{tr}) - \frac{1}{\tau_p} \right] E + \kappa E_{inj} - i2\pi\Delta f E \quad (1)$$

where E is the complex field of the injection-locked slave laser, α is the linewidth enhancement factor, G is the linear gain coefficient, N is the carrier number, N_{tr} is the transparency carrier number, τ_p is the photon lifetime, κ is the coupling rate, E_{inj} is the complex field of the master laser, and Δf is the frequency difference between the master laser and the free-running (FR) slave laser (detuning frequency [10]). Note that the spontaneous emission is ignored in (1). The linear gain coefficient G is defined by

$$G = \frac{\Gamma g v_g}{V} \quad (2)$$

where g is the differential gain coefficient, v_g is the group velocity, and V is the active region volume. In order to obtain simple analytical expressions, the nonlinear gain compression effect is not considered here. From (1), we can derive the rate equations for photon number and phase, by defining the optical field as

$$E = \sqrt{S} e^{i\theta}, \quad E_{inj} = \sqrt{S_{inj}} e^{i\theta_{inj}} \quad (3)$$

where S and θ describe the photon number and phase for the slave laser, and S_{inj} and θ_{inj} describe the photon number and phase for the master laser, respectively. Substituting (3) into (1) and following the derivative method in [17], we can obtain the rate equations for photon number and phase:

$$\frac{dS}{dt} = \left[G(N - N_{tr}) - \frac{1}{\tau_p} \right] S + 2\kappa \sqrt{S_{inj}} S \cos(\theta - \theta_{inj}) \quad (4)$$

$$\frac{d\theta}{dt} = \frac{\alpha}{2} \left[G(N - N_{tr}) - \frac{1}{\tau_p} \right] - 2\pi\Delta f - \kappa \sqrt{\frac{S_{inj}}{S}} \sin(\theta - \theta_{inj}). \quad (5)$$

The carrier number rate equation is given by [20]

$$\frac{dN}{dt} = \eta_i \frac{I}{q} - \frac{N}{\tau_s} - G(N - N_{tr}) S \quad (6)$$

where η_i is the internal quantum efficiency, I is the injected current, q is the electron charge, and τ_s is the carrier lifetime. Equations (4)–(6) constitute the three differential rate equations for OIL lasers. In principle, many parameters on the right-hand sides of (4)–(6) can be modulated. For example, both the amplitude and phase of the master laser can be modulated by an additional modulator before injection [21], which is called master modulation. In the present work, we will consider applying modulation signals directly to the slave laser, specifically the OIL laser is only subject to the modulation of I and τ_p separately.

2.2. Derivation of Frequency Response

Using standard small-signal analysis, the dynamic photon number, phase, and carrier number can be written as the sum of a dc component and a sinusoidal perturbation

$$S = S_0 + \Delta S e^{j\omega t}, \quad \theta = \theta_0 + \Delta\theta e^{j\omega t}, \quad N = N_0 + \Delta N e^{j\omega t} \quad (7)$$

where $\Delta S \ll S_0$, $\Delta\theta \ll \theta_0$, and $\Delta N \ll N_0$. For conventional current modulation, the current can be written as

$$I = I_0 + \Delta I e^{j\omega t} \quad (8)$$

where $\Delta I \ll I_0$. Substituting (7) and (8) into (4)–(6), linearizing, and then separating the dc and sinusoidal perturbation parts yields the steady state and small-signal solutions. We can then describe the small-signal solutions in a compact matrix form [10]

$$\begin{bmatrix} m_{SS} + j\omega & m_{S\theta} & m_{SN} \\ m_{\theta S} & m_{\theta\theta} + j\omega & m_{\theta N} \\ m_{NS} & 0 & m_{NN} + j\omega \end{bmatrix} \begin{bmatrix} \Delta S \\ \Delta\theta \\ \Delta N \end{bmatrix} = \begin{bmatrix} 0 \\ 0 \\ \eta_i \Delta I / q \end{bmatrix} \quad (9)$$

where the terms in the first (left) matrix T are

$$\begin{aligned} m_{SS} &= z \cos(\theta_0 - \theta_{inj}), & m_{S\theta} &= 2zS_0 \sin(\theta_0 - \theta_{inj}), & m_{SN} &= -GS_0 \\ m_{\theta S} &= -z \sin(\theta_0 - \theta_{inj}) / 2S_0, & m_{\theta\theta} &= z \cos(\theta_0 - \theta_{inj}), & m_{\theta N} &= -\alpha G / 2 \\ m_{NS} &= 1 / \tau_p - 2z \cos(\theta_0 - \theta_{inj}), & & & m_{NN} &= 1 / \tau_s + GS_0 \end{aligned} \quad (10)$$

and $z = \kappa \sqrt{S_{inj} / S_0}$. We can rearrange (9) as

$$\begin{bmatrix} \Delta S \\ \Delta\theta \\ \Delta N \end{bmatrix} = T^{-1} \begin{bmatrix} 0 \\ 0 \\ \eta_i \Delta I / q \end{bmatrix} \quad (11)$$

where the left-hand side represents the output terms, and the last matrix on the right-hand side represents the input terms. Then, we can obtain the amplitude frequency response for current modulation:

$$H(\omega) = \frac{\Delta S}{\Delta I} = M \frac{j\omega + D}{(j\omega)^3 + A(j\omega)^2 + B(j\omega) + C} \quad (12)$$

where

$$\begin{aligned} A &= m_{SS} + m_{\theta\theta} + m_{NN}, & B &= m_{SS}m_{\theta\theta} + m_{SS}m_{NN} + m_{\theta\theta}m_{NN} - m_{S\theta}m_{\theta S} - m_{SN}m_{NS} \\ C &= m_{SS}m_{\theta\theta}m_{NN} + m_{S\theta}m_{\theta N}m_{NS} - m_{S\theta}m_{\theta S}m_{NN} - m_{SN}m_{NS}m_{\theta\theta} \\ D &= (m_{SN}m_{\theta\theta} - m_{S\theta}m_{\theta N}) / m_{SN}, & M &= -m_{SN}\eta_i / q. \end{aligned} \quad (13)$$

For Q-modulation, the photon lifetime can be written as

$$\frac{1}{\tau_p} = \frac{1}{\tau_{p0}} + \frac{1}{\Delta\tau_p} e^{j\omega t} \quad (14)$$

where $\Delta\tau_p \gg \tau_{p0}$. Substituting (7) and (14) into (4)–(6), we can get the small-signal solutions in the matrix form similar to (9)

$$\begin{bmatrix} m_{SS} + j\omega & m_{S\theta} & m_{SN} \\ m_{\theta S} & m_{\theta\theta} + j\omega & m_{\theta N} \\ m_{NS} & 0 & m_{NN} + j\omega \end{bmatrix} \begin{bmatrix} \Delta S \\ \Delta\theta \\ \Delta N \end{bmatrix} = \begin{bmatrix} -S_0 / \Delta\tau_p \\ -\alpha / 2\Delta\tau_p \\ 0 \end{bmatrix} \quad (15)$$

where the first matrix is the same as T described in (10). Similarly, we can rearrange (15) as

$$\begin{bmatrix} \Delta S \\ \Delta\theta \\ \Delta N \end{bmatrix} = T^{-1} \begin{bmatrix} -S_0 / \Delta\tau_p \\ -\alpha / 2\Delta\tau_p \\ 0 \end{bmatrix} \quad (16)$$

then we can obtain the amplitude frequency response for Q-modulation

$$H(\omega) = \frac{\Delta S}{1 / \Delta\tau_p} = M' \frac{(j\omega + D)(j\omega + E)}{(j\omega)^3 + A(j\omega)^2 + B(j\omega) + C} \quad (17)$$

where A , B , C , and D are the same as in (13), and the other terms are given as follows:

$$E = m_{NN}, \quad M' = -S_0. \quad (18)$$

2.3. Comparison of Frequency Response

From (12) and (17), we can see that the two modulation methods share the same denominator in their frequency response, which can be factored into its corresponding poles [10]

$$(j\omega)^3 + A(j\omega)^2 + B(j\omega) + C = (j\omega + \omega_P) \left(j\omega - j\omega_R + \frac{\gamma}{2} \right) \left(j\omega + j\omega_R + \frac{\gamma}{2} \right) \quad (19)$$

where ω_P is the real-pole frequency, ω_R is the resonance frequency, and γ is the damping factor. This indicates that Q-modulation has the same resonance frequency as current modulation, which can be approximated by [12]

$$\omega_R^2 \approx -m_{SN}m_{NS} - m_{S\theta}m_{\theta S} \approx \omega_{R0}^2 + \Delta\omega_R^2 \quad (20)$$

where ω_{R0} is the resonance frequency of FR lasers

$$\omega_{R0} = \sqrt{\frac{GS_0}{\tau_p}} \quad (21)$$

and $\Delta\omega_R$ can be regarded as the resonance frequency enhancement by injection locking

$$\Delta\omega_R = \left| \kappa \sqrt{\frac{S_{inj}}{S_0}} \sin(\theta_0 - \theta_{inj}) \right| = \left| 2\pi\Delta f - \frac{\alpha}{2} \left[G(N_0 - N_{tr}) - \frac{1}{\tau_p} \right] \right|. \quad (22)$$

From (22), we can see that $\Delta\omega_R$ is equal to the frequency difference between the master laser and the shifted cavity mode of the slave laser [22]. As discussed in [10], the resonance frequency increases with increasing injection ratio and/or detuning frequency. This will also be illustrated in Section 3.

For sufficiently large positive detuning frequencies and injection ratios ($\Delta\omega_R \gg \omega_{R0}$), $|D|$ is much larger than ω_R [21]; therefore, the term $(j\omega + D)$ on the numerator of (12) and (17) tends to have little effect on the frequency response, except for very high frequencies. The real-pole frequency ω_P is much less than ω_R and can be approximated by [10]

$$\omega_P \approx \frac{C}{\omega_R^2} \approx \frac{1}{\tau_s} + \left[1 + \frac{\alpha}{\omega_R} G(N_0 - N_{tr}) \right] GS_0. \quad (23)$$

For current modulation, ω_P causes a roll-off at frequencies between dc and ω_R that can severely limit the 3-dB bandwidth. However, for Q-modulation, the additional term $(j\omega + E)$ on the numerator of (17) will play an important role. We can expand E , using (10)

$$E = m_{NN} = \frac{1}{\tau_s} + GS_0. \quad (24)$$

By comparing (23) with (24), we can see that E is slightly smaller than ω_P ; therefore, the dc-to-resonance roll-off can be largely cancelled. On the other hand, at high frequencies, the existence of the term $(j\omega + E)$ implies that the frequency response of Q-modulation decays slower than that of current modulation, in a similar way as in the case of FR lasers [9]. As a result, the 3-dB bandwidth can be significantly enhanced beyond the resonance frequency. We can also approximate the Q-modulation response in (17) for frequencies sufficiently high above E and ω_P but well below $|D|$ to

$$H(\omega) \approx \frac{|DM'|}{\omega_R^2 - \omega^2 + j\gamma\omega} \quad (25)$$

which resembles the classic double-pole frequency response of FR lasers under direct current modulation [2] but with a greatly enhanced resonance frequency.

2.4. Physical Origin and Chirp

From the analytical formulas that we derived above, it is expected that the frequency response of OIL lasers can be even further improved using Q-modulation as compared with current modulation. Here, we explore its physical origin. In FR lasers, the resonance frequency is determined by the dynamic coupling between carriers and photons, as can be seen in (20), where the term $-m_{SN}m_{NS}$ corresponds to the FR resonance frequency ω_{R0} . For OIL lasers, the dynamic coupling between photons and phase becomes dominant [10]. This can be seen in (20), where the term $-m_{S\theta}m_{\theta S}$ corresponds to the resonance frequency enhancement $\Delta\omega_R$, and $\Delta\omega_R$ is typically much larger than ω_{R0} for high injection ratios and large positive detuning frequencies. For OIL current-modulated lasers (OIL-CMLs), the modulation signal is first transferred to the carriers, but the carriers lie outside of the dominant resonance dynamics (resonance between photons and phase), hence the modulation speed is bottlenecked by the rate in which the carriers can transfer information to the photons and phase [21]. This rate is related to the real-pole frequency ω_P , thus resulting in the dc-to-resonance roll-off. Additionally, this causes the response to decay as $1/\omega^3$ at high frequencies beyond the resonance. For OIL Q-modulated lasers (OIL-QMLs), the modulation signal is directly applied to the photons and phase, and the carrier number variation can be regarded as a by-product. Hence, the dc-to-resonance roll-off is largely eliminated. The frequency response also tends to resemble the classic double-pole frequency response as in FR current-modulated lasers (FR-CMLs), but with a much larger resonance frequency (resonance between photons and phase rather than between photons and carriers). Furthermore, at frequencies beyond the resonance, the response decay rate returns to $1/\omega^2$.

We can also derive the relationship between ΔN and ΔS for OIL-QML using (15)

$$\frac{\Delta N}{\Delta S} = \frac{-m_{NS}}{m_{NN} + j\omega}. \quad (26)$$

From (26), we can see that for a given modulation depth (ΔS), the variation of carrier number decreases as $1/\omega$ for increasing frequency. This is similar to the case of FR Q-modulated lasers (FR-QMLs) [9], and again, verifies that ΔN is a by-product of ΔS in Q-modulation, rather than the driving force for ΔS as in current modulation. In FR lasers, this will lead to a much lower chirp at high frequencies for Q-modulation, since the chirp is proportional to ΔN .

However, the chirp characteristic of OIL lasers is very different from that of FR lasers and has been studied by several authors [10], [23], [24]. An important figure-of-merit for chirp is the chirp-to-power ratio (CPR), which is defined as the ratio of lasing frequency deviation to power deviation. Here, we derive the CPR for OIL-QML to be

$$\text{CPR} = \left| j\omega \frac{\Delta\theta}{\Delta S} \right| = \frac{\alpha}{2S_0} \left| j\omega \frac{j\omega + \omega_A}{j\omega + \omega_B} \right| \quad (27)$$

where

$$\omega_A = z [\cos(\theta_0 - \theta_{inj}) + \sin(\theta_0 - \theta_{inj})/\alpha], \quad \omega_B = z [\cos(\theta_0 - \theta_{inj}) - \alpha \sin(\theta_0 - \theta_{inj})]. \quad (28)$$

The expression for CPR in (27) is exactly the same as in [10] for OIL-CML, except that the gain compression is neglected in this derivation. Therefore, we can expect that Q-modulation has the same chirp characteristics as current modulation for OIL lasers. This is consistent with the fact that CPR is only determined by the dynamic coupling between photons and phase [see (4) and (5)], regardless of how the modulation enters the coupling (i.e., either through $G(N - N_{tr})$ in current modulation or through τ_p in Q-modulation). The situation is different in FR lasers and can be explained since CPR is actually proportional to $|\Delta N/\Delta S|$, which depends on the modulation method.

TABLE 1
List of simulation parameters

Symbol	Value	Units
α	4	
Γ	0.04	
g	1×10^{-15}	cm^2
v_g	8.8	cm/ns
V	2.5×10^{-12}	cm^3
N_{tr}	1.2×10^6	
τ_{p0}	10	ps
κ	100	ns^{-1}
η_i	0.5	
τ_s	0.4	ns

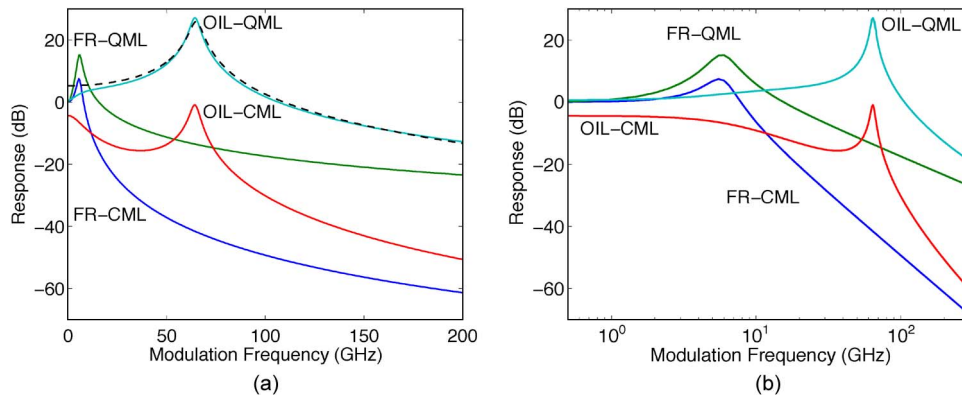


Fig. 1. Modulation frequency response comparison. (a) Frequency on linear scale, (b) frequency on logarithmic scale. The threshold current (I_{th}) of the FR laser is 1.53 mA, and the dc bias current is kept at $3 \times I_{th}$. For the OIL laser, the injection ratio is 15 dB, and the detuning frequency is 50 GHz. The responses are normalized that the FR responses are at 0 dB at dc. The dashed curve in (a) is the frequency response for OIL-QML approximated using (25), and all other curves in (a) and (b) are obtained numerically. In (b), the response decay rate beyond resonance frequency is 40, 20, 60, and 40 dB/dec for FR-CML, FR-QML, OIL-CML, and OIL-QML, respectively.

3. Numerical Simulations

In this section, we present the numerical simulation results for the proposed Q-modulation of OIL lasers. Table 1 lists the parameters used in the simulations. To obtain the small-signal frequency response, we first bias the laser and allow it to stabilize (for OIL lasers, it should be within the locking range) and then apply a small sinusoidal modulation to the pumping current or the photon lifetime. We determine the oscillation amplitude of the photon number and then repeat this for different modulation frequencies.

Fig. 1 shows the normalized frequency response for the four cases: FR-CML, FR-QML, OIL-CML, and OIL-QML. For the FR laser, CML and QML have the same resonance frequency (5.5 GHz), but QML has a higher response at the resonance frequency [9], and the response decays much slower beyond the resonance frequency; therefore, QML has a much larger 3-dB bandwidth (20.5 GHz) than CML (9 GHz). When the laser is injection-locked, the resonance frequency is greatly enhanced up to 64 GHz for both CML and QML. From the response of OIL-CML, we can see that there is a large roll-off between dc and resonance frequency, which limits the 3-dB bandwidth well below the resonance frequency (only about 7 GHz); besides, the decay rate beyond the resonance frequency is the fastest among the four cases (60 dB/dec, corresponding to $1/\omega^3$). For the case of OIL-QML,

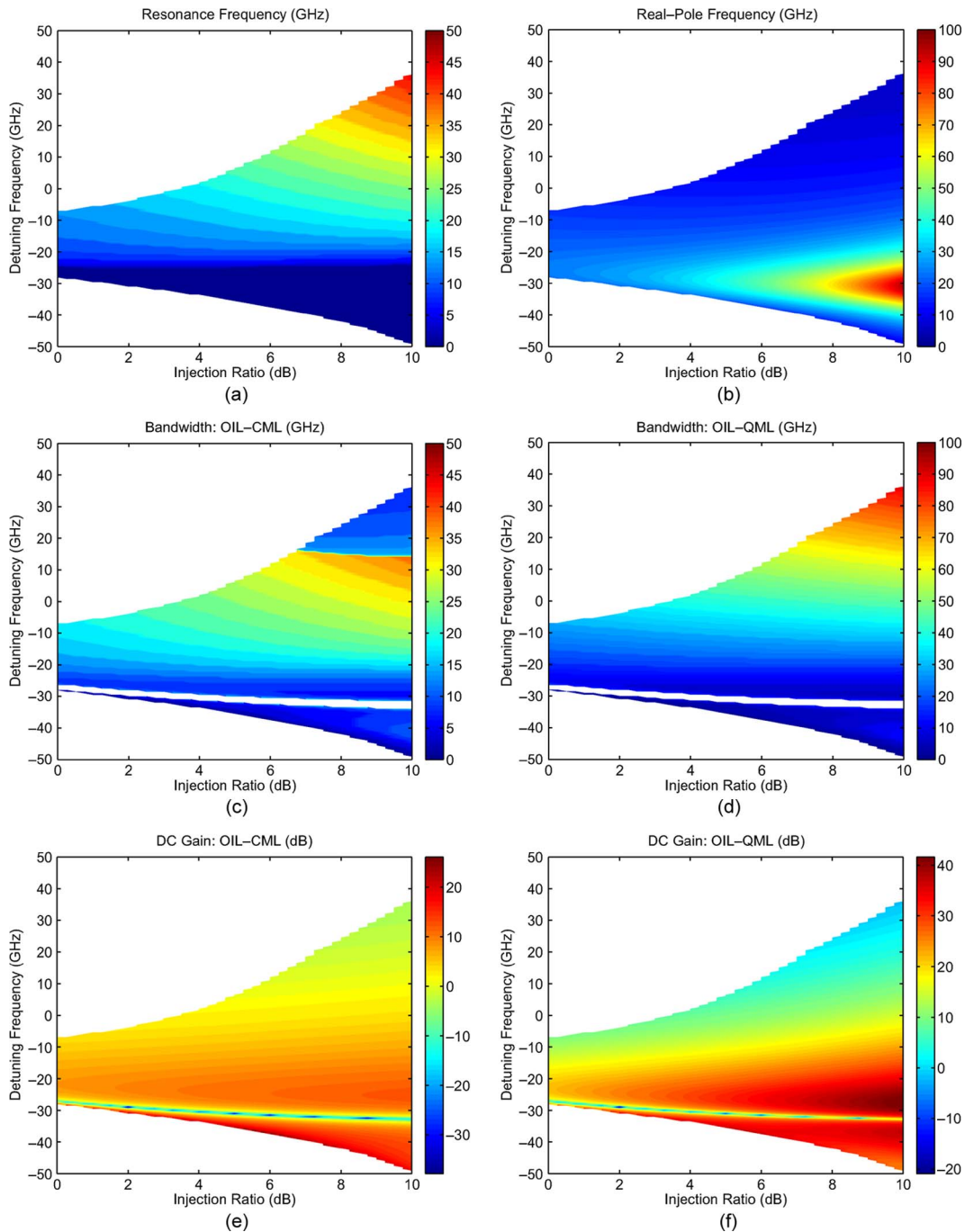


Fig. 2. Contour plot across the locking range for (a) resonance frequency, (b) real-pole frequency, (c) OIL-CML bandwidth, (d) OIL-QML bandwidth, (e) OIL-CML dc gain, and (f) OIL-QML dc gain. The dc gain is defined as the ratio between the OIL response and the FR response at dc.

we do not see the dc-to-resonance roll-off, agreeing with our expectation that the $(j\omega + E)$ and $(j\omega + \omega_p)$ terms will almost cancel each other out. The tiny dip at very low frequencies around dc is due to the fact that E is slightly smaller than ω_p . This can be explained that at very low frequencies, the carriers try to catch up with the photons' modulation, as can be seen from (26), and affect the "pure" dynamic coupling between photons and phase, thus slightly slowing down the system's response to the Q-modulation. Otherwise, the response resembles the double-pole frequency

response of FR-CML, with the benefit of the enhanced resonance frequency. This is also validated by comparing the numerically simulated response (solid curve) with the approximated response using (25) (dashed curve) in Fig. 1(a). Note that the latter response is obtained by fixing the OIL laser at steady state and then extracting all the parameters needed for (25). Beyond the resonance frequency, the response decays at the same rate as in FR-CML (i.e., 40 dB/dec, corresponding to $1/\omega^2$); therefore, the 3-dB bandwidth is well above the resonance frequency (117 GHz).

In order to perform a more comprehensive study, we simulate the frequency response for different values of injection ratio and detuning frequency across the locking range. From Fig. 2(a), we see that the resonance frequency increases with increasing injection ratio and/or detuning frequency. However, the region of largest resonance frequency corresponds to very low real-pole frequencies in Fig. 2(b), resulting in the abrupt drop in the 3-dB bandwidth of OIL-CML, as shown in Fig. 2(c). In contrast, the 3-dB bandwidth of OIL-QML is not limited by the real-pole frequency; therefore, the 3-dB bandwidth has the similar trend as the resonance frequency, i.e., the largest bandwidth occurs at the positive detuning edge and high injection ratios. From Fig. 2(d), we can also see that the bandwidth is almost twice the resonance frequency, again indicating that the bandwidth can be enhanced well above the resonance frequency.

It is interesting to note that there is a narrow blank band on the negative detuning side in both Fig. 2(c) and (d), which corresponds to the discontinuous area in Fig. 2(e) and (f), where the dc gain suddenly drops. Within this area, the zero-frequency D approaches zero:

$$\cos(\theta_0 - \theta_{inj}) \approx \alpha \sin(\theta_0 - \theta_{inj}) \quad (29)$$

and causes a very sharp dip in the modulation response at dc. Similar to the discussion in [13], this abnormality corresponds to the transition of data pattern inversion, i.e., the data pattern goes through a transition from a non-inverted to an inverted state as the detuning frequency crosses the narrow band (from positive to negative frequency detuning).

4. Conclusion

We have proposed Q-modulation of an optically injection-locked semiconductor laser. The rate equation model for OIL lasers is used to analyze the small-signal frequency response, for both current modulation and Q-modulation. We find that the two modulation methods have the same resonance frequency. However, using Q-modulation, the dc-to-resonance roll-off caused by the real-pole frequency is largely cancelled, and above the resonance frequency, the response decays as $1/\omega^2$, in contrast to $1/\omega^3$ using current modulation. As a result, a significant enhancement in the 3-dB bandwidth is achieved. We can also approximate the frequency response to the classic double-pole frequency response of conventional current modulation of FR lasers, although the resonance frequency is greatly increased. Furthermore, we explain that the frequency response improvements are due to the fact that the modulation of Q directly enters the dynamic coupling between photons and phase, and the carrier number variation can be regarded as a by-product. Finally, we expect that Q-modulation will have similar chirp characteristics as using current modulation for OIL lasers.

References

- [1] Y. Suematsu and K. Iga, "Semiconductor lasers in photonics," *J. Lightw. Technol.*, vol. 26, no. 9, pp. 1132–1144, May 2008.
- [2] L. A. Coldren and S. W. Corzine, *Diode Lasers and Photonic Integrated Circuits*. New York: Wiley, 1995.
- [3] V. B. Gorfinkel and S. Luryi, "High-frequency modulation and suppression of chirp in semiconductor lasers," *Appl. Phys. Lett.*, vol. 62, no. 23, pp. 2923–2925, Jun. 1993.
- [4] A. Frommer, S. Luryi, D. T. Nichols, J. Lopata, and W. S. Hobson, "Direct modulation and optical confinement factor modulation of semiconductor lasers," *Appl. Phys. Lett.*, vol. 67, no. 12, pp. 1645–1647, Sep. 1995.
- [5] E. A. Avrutin, V. B. Gorfinkel, S. Luryi, and K. A. Shore, "Control of surface-emitting laser diodes by modulating the distributed Bragg mirror reflectivity: Small-signal analysis," *Appl. Phys. Lett.*, vol. 63, no. 18, pp. 2460–2462, Nov. 1993.
- [6] S. Dods and M. Ogura, "Q-modulation of a surface emitting laser and an integrated detuned cavity," *IEEE J. Quantum Electron.*, vol. 30, no. 5, pp. 1204–1211, May 1994.

- [7] J.-J. He, "Proposal for Q-modulated semiconductor laser," *IEEE Photon. Technol. Lett.*, vol. 19, no. 5, pp. 285–287, Mar. 2007.
- [8] D. Dai, A. Fang, and J. E. Bowers, "Hybrid silicon lasers for optical interconnects," *New J. Phys.*, vol. 11, no. 125016, pp. 1–17, 2009.
- [9] D. Liu, L. Wang, and J.-J. He, "Rate equation analysis of high speed Q-modulated semiconductor laser," *J. Lightw. Technol.*, vol. 28, no. 21, pp. 3128–3135, Nov. 2010.
- [10] E. K. Lau, L. J. Wong, and M. C. Wu, "Enhanced modulation characteristics of optical injection-locked lasers: A tutorial," *IEEE J. Sel. Topics Quantum Electron.*, vol. 15, no. 3, pp. 618–633, May/Jun. 2009.
- [11] E. K. Lau, X. Zhao, H.-K. Sung, D. Parekh, C. Chang-Hasnain, and M. C. Wu, "Strong optical injection-locked semiconductor lasers demonstrating > 100-GHz resonance frequencies and 80-GHz intrinsic bandwidths," *Opt. Express*, vol. 16, no. 9, pp. 6609–6618, Apr. 2008.
- [12] E. K. Lau, H. K. Sung, and M. C. Wu, "Frequency response enhancement of optical injection-locked lasers," *IEEE J. Quantum Electron.*, vol. 44, no. 1, pp. 90–99, Jan. 2008.
- [13] X. Zhao, B. Zhang, L. Christen, D. Parekh, W. Hofmann, M. C. Amann, F. Koyama, A. E. Willner, and C. J. Chang-Hasnain, "Greatly increased fiber transmission distance with an optically injection-locked vertical-cavity surface-emitting laser," *Opt. Express*, vol. 17, no. 16, pp. 13 785–13 791, Aug. 2009.
- [14] L. Chrostowski, X. Zhao, and C. Chang-Hasnain, "Microwave performance of optically injection-locked VCSELs," *IEEE Trans. Microw. Theory Tech.*, vol. 54, no. 2, pp. 788–796, Feb. 2006.
- [15] H.-K. Sung, E. K. Lau, and M. C. Wu, "Optical single sideband modulation using strong optical injection-locked semiconductor lasers," *IEEE Photon. Technol. Lett.*, vol. 19, no. 13, pp. 1005–1007, Jul. 2007.
- [16] R. Lang, "Injection locking properties of a semiconductor laser," *IEEE J. Quantum Electron.*, vol. QE-18, no. 6, pp. 976–983, Jun. 1982.
- [17] L. Chrostowski, B. Faraji, W. Hofmann, M.-C. Amann, S. Wiczorek, and W. W. Chow, "40 GHz bandwidth and 64 GHz resonance frequency in injection-locked 1.55 μm VCSELs," *IEEE J. Sel. Topics Quantum Electron.*, vol. 13, no. 5, pp. 1200–1208, Sep./Oct. 2007.
- [18] J. Troger, P.-A. Nicati, L. Thevenaz, and P. A. Robert, "Novel measurement scheme for injection-locking experiments," *IEEE J. Quantum Electron.*, vol. 35, no. 1, pp. 32–38, Jan. 1999.
- [19] S. Wiczorek, W. W. Chow, L. Chrostowski, and C. J. Chang-Hasnain, "Improved semiconductor-laser dynamics from induced population pulsation," *IEEE J. Quantum Electron.*, vol. 42, no. 6, pp. 552–562, Jun. 2006.
- [20] L. Chrostowski and W. Shi, "Monolithic injection-locked high-speed semiconductor ring lasers," *J. Lightw. Technol.*, vol. 26, no. 19, pp. 3355–3362, Oct. 2008.
- [21] E. K. Lau, L. J. Wong, X. Zhao, Y.-K. Chen, C. J. Chang-Hasnain, and M. C. Wu, "Bandwidth enhancement by master modulation of optical injection-locked lasers," *J. Lightw. Technol.*, vol. 26, no. 15, pp. 2584–2593, Aug. 2008.
- [22] A. Murakami, K. Kawashima, and K. Atsuki, "Cavity resonance shift and bandwidth enhancement in semiconductor lasers with strong light injection," *IEEE J. Quantum Electron.*, vol. 39, no. 10, pp. 1196–1204, Oct. 2003.
- [23] S. Piazzolla, P. Spano, and M. Tamburrini, "Small signal analysis of frequency chirping in injection-locked semiconductor lasers," *IEEE J. Quantum Electron.*, vol. QE-22, no. 12, pp. 2219–2223, Dec. 1986.
- [24] G. Yabre, "Effect of relatively strong light injection on the chirp-to-power ratio and the 3 dB bandwidth of directly modulated semiconductor lasers," *J. Lightw. Technol.*, vol. 14, no. 10, pp. 2367–2373, Oct. 1996.